Comparison of rockfall models using photogrammetry to data from an experimental Smart Rock

Corinne Disenhof
University of New Hampshire Department of Civil Engineering, Durham, NH, USA, crc8@wildcats.unh.edu

Jean Benoît
University of New Hampshire Department of Civil Engineering, Durham, NH, USA, jean.benoit@unh.edu

Artur Apostolov
Geocomp Corporation, Acton, MA, USA, aapostolov@geocomp.com

Krystle Pelham, Neil Olson
New Hampshire Department of Transportation, Concord, NH, USA, krystle.pelham@dot.nh.gov, neil.olson@dot.nh.gov

ABSTRACT: Rockfall is a worldwide problem, claiming lives and causing damage to infrastructure. Though common and well-studied in mountainous areas, it poses hazards in less rugged terrain as well, where detailed assessments of rock slope stability are rare. Detailed digital data for use in rockfall modeling can be expensive to obtain. The University of New Hampshire is examining the use of an instrumented "Smart Rock" for in-situ rockfall characterization in combination with rockfall modeling using easily-obtainable photogrammetry models. Smart Rock measurements characterize the rotational velocity and acceleration of a rock throughout an experimental rockfall. Comparison of experimental data to 2D rockfall models shows that a Smart Rock can be used to verify model results, and that photogrammetry models created using simple methodologies can successfully model rockfall.

Keywords: rockfall; modeling; Smart Rock; photogrammetry

1. Introduction

Rockfall is a hazard throughout the world. In the United States, millions of dollars are spent annually to prevent falling rocks from threatening lives and property [1]. Experimental and theoretical methods are used to assess rockfall hazards to aid in the design of engineered protective structures. However, real rockfall data for use in design are limited.

Full scale rockfall experiments and computer simulations are the primary ways of predicting rockfall hazards, including falling rock trajectories and impact velocities. Duffy and Turner [2] provide a comprehensive list of rockfall experiments conducted between 1963 and 2009. Experimental rockfalls can be used to determine the trajectories, bounce heights, and velocities of falling rocks. Computer simulations use digital representations of rock slopes and mathematical models to predict the motion of falling rocks. However, for these models to present accurate results, they need to be calibrated with data specific to the modeled location, such as detailed slope geometry and material properties.

In approximately the last decade, universities and research groups world-wide, including the University of New Hampshire (UNH), have developed sensors contained in sealed protective containers, intended to investigate and monitor soil and rock movement from the interior of a slope failure event. UNH began development of a "Smart Rock" in the 2000s and has produced a small, autonomous instrument capable of monitoring the movement of a rock during rockfall [3-6].

This paper compares data from an instrumented Smart Rock used in experimental rockfalls conducted in New Hampshire, USA to digital rockfall models created from 3-dimensional (3D) surficial models of the experimental rock slopes. The Smart Rock was used to record the motion of falling rocks in order to evaluate the applicability of the Smart Rock for comparison to and verification of rockfall models. Digital rockfall models were created using photogrammetry data sets, created in one location by professional photogrammetry using an Unmanned Aerial System (UAS) and in a second location, by simple, easily obtained photos taken by a handheld camera.

1.1. University of New Hampshire Smart Rock

Instrumented rocks in use around the world typically include 3-axis accelerometers and gyroscopes. The reader is referred to [3-9] for discussion of instruments in use by other universities and research groups.

UNH's third generation Smart Rock (SR) was developed by Apostolov [3, 6]. Though UNH's original SRs were developed to track soil particles in debris flow flume experiments [4, 5, 10], the third-generation SR now includes a version suitable for rockfall experiments, shown with its protective shell in Fig. 1.

The rockfall-specific SR measures 3D acceleration using ±400 g and ±16 g accelerometers, as well as rotational velocity using a ±4000 degrees per second (dps) high-rate gyroscope [3, 6]. The ±16 g accelerometer can be set to read ±2 g, ±4 g, or ±16 g as

desired; in this study, it was limited to ±8 g in order to decrease noise in the acceleration signal. Data are acquired at a frequency of 500Hz, which was previously determined to be sufficient for these dynamic experiments, and the data are written to a micro SD card. The outputs of this SR are measurements of 3D acceleration and rotational velocity [6]. The rockfall SR is protected using a 2.54 cm diameter, 4.2 cm long custom 3D printed plastic shell, as shown in Fig. 1. The mass of the instrument and shell is 22.5 g. For rockfall experiments, the SR is secured inside a natural stone using an expandable rubber plug, and the stone is subsequently dropped or rolled off the study slope. The rock is prepared by drilling a hole with a 2.54 cm outer diameter core bit to a depth of at least 7.5 cm, in order to accommodate both the SR and the seal plug [11].

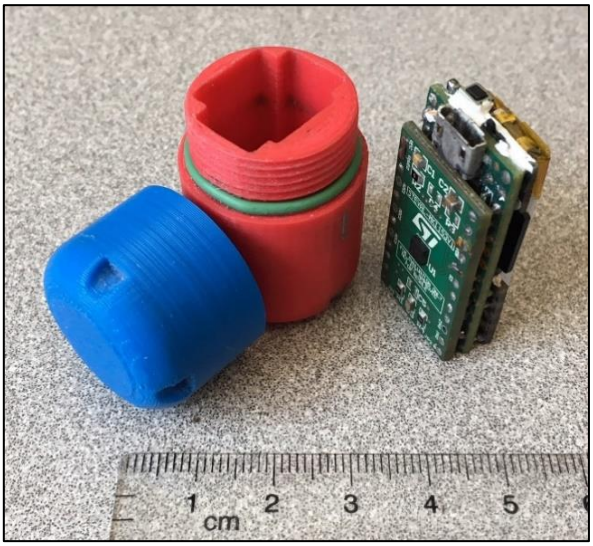

Figure 1. The rockfall Smart Rock sensor and protective shell.

1.2. Rockfall Models

Smart Rock data from experimental rockfalls at two highway rock cuts in New Hampshire (NH), USA were compared against rockfall models created using Rocscience's RocFall software [12]. RocFall simulates a modeled rock falling down a slope defined by the user, with the motion of the rock mathematically determined based on the characteristics of the slope surface and the modeled rock. In this study, rigid body analyses were performed to take the shape of the rock into account as well as the mass and size. The slope characteristics are defined by the total energy coefficient of restitution (R_E), the ratio of the final (post-impact) to initial (pre-impact) total kinetic energies of the falling rock [7, 13, 14], and dynamic and rolling friction coefficients (μ and μ_r, respectively) [15-17]. Coefficients of restitution used in this study are drawn from coefficients provided by [18] and listed in Table 1. Rocscience's [18] default coefficients of restitution do not provide values of R_E, however, research by [13] and [16] indicates that values of R_E are similar to the ratio of final to initial velocities of a rock impacting normal to the slope, which is the normal coefficient of restitution, R_N. Values of R_N were used here.

The 2-dimensional slope models used in the rockfall simulations were extracted from 3D surface models generated by photogrammetry for each rock cut. One rock cut, in Derry, NH, was imaged using a handheld camera and modeled using a simple structure from motion (SfM) photogrammetry procedure, which is described in [11]. In July 2017, the New Hampshire Department of Transportation (NHDOT), in conjunction with the University of Vermont, flew a UAS to capture images of a second rock slope in Hart's Location, NH and create a professional 3D model using SfM. The data were made available to UNH for this research by the NHDOT.

Table 1. Coefficients of restitution used in computational models, identified by color on the figures in this text. Where coefficients or standard deviations did not accompany the primary table entry, values were applied using program defaults.

Color	Description	R_N	μ	μ_r	Source
	Bedrock outcrops	0.35±0.04	0.55±0.04	0.15±0.04	[18]
	Talus Cover	0.32±0.04	0.55±0.04	0.3±0.04	[18]
	Soft soil, some vegetation	0.30±0.06	0.55±0.04	0.3±0.02	[18]
	Asphalt	0.40±0.04	0.55±0.04	0.1±0.01	[18]

2. Smart Rock Experiments

Rockfall experiments were performed to test the application of the new rockfall SR for direct measurement of acceleration and rotation during rockfall. These measurements, along with video taken of each test and measured rock runout, the farthest distance traveled by each falling rock, provided data for comparison to digital rockfall models.

In April and May, 2018, the NHDOT Bureau of Materials and Research provided access to two rock cuts while they were undergoing hand scaling to remove loose rock. The first site was on Interstate 93 (I-93) in Derry, NH. This rock cut was newly blasted and the catchment ditch was not yet constructed at the time of testing. The second site was at a rock cut in Hart's Location, NH, near Crawford Notch, which is considered one of the more hazardous rock cuts in New Hampshire [19].

2.1. Rocks

The rocks used for experimental rockfalls with the SR were natural rocks chosen based on durability and size, such that they could be easily transported by hand or hoisted to the top of a slope. The same rocks were used for all experiments.

The rocks used were a 5.3 kg sub-angular metamorphic rock (rock 1) and a 10.8 kg angular, blocky diorite (rock 2), both shown in Fig. 2. The characteristics of each rock are provided in Table 2. Holes were drilled in the test rocks to accommodate the SR. Though placement of the SR at the centroid of the rock shape is ideal, due to the constraints of the drill, the hole in the rock 2 had to be offset. For comparison of rock motion to recent results from [9], the mass moments of inertia were estimated for each axis of the

two rocks, which are shown in Table 3. These are oriented with respect to the orientation of the SR within each test rock, which are shown in Fig. 2.

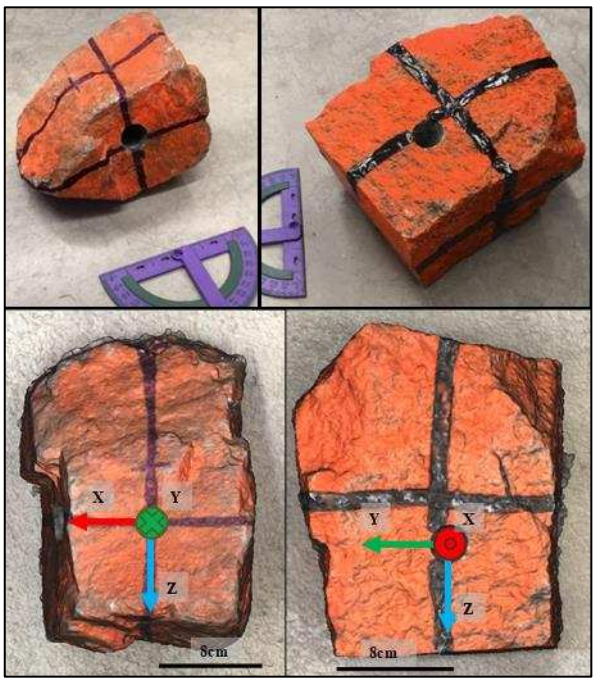

Figure 2. Top: Rocks used for experimental rockfalls, with rock 1 on the left and rock 2 on the right. Bottom: the orientation of the SR within the rocks.

Table 2. Characteristics of rocks used in field experiments. The Smart Rock (X, Y, Z) axes shown in Fig. 2 correspond to the height, width, and length measurements, respectively.

Rock	L (cm)	W (cm)	H (cm)	Mass (kg)	Density (kg/m^3)
1	20	12	12	5.30	2660
2	20.3	17	12.5	10.83	2770

Table 3. Estimated mass moments of inertia (I) for each test rock

Rock	Mass Moment of Inertia (kg·m^2)		
	I_{XX}	I_{YY}	I_{ZZ}
1	0.024	0.024	0.013
2	0.063	0.051	0.040

2.2. Derry, NH

2.2.1. Rock cut and experimental procedure

The highway rock cut used for rockfall experiments in Derry, NH is approximatley 15 m tall and newly created. The rock cut is shown in Fig. 3. The rock face at this location has an approximately 70 degree slope. No engineered protective ditch had been created at the time of the experiments, but a small talus slope with an approximately 4 m wide, 0.5 m deep rock-lined ditch existed at the foot of the slope. Hand scaling of the cut to remove loose rock was in progress during SR testing, and the test rocks were dropped in this location by scalers with rope access to the top of the slope.

Seven experimental rockfalls were conducted at this site: three with the approximately 5 kg rock 1 and four with the approximatley 11 kg rock 2. All three tests with rock 1 and one with rock 2 obtained SR data. Test trials 4, 5, and 6 did not record data due to the start switch being inadvertently turned off while inserting the sealing plug. Newer generations of the SR have now fixed this issue.

The SR was inserted into the test rocks at the bottom of the slope and pulled up the rock face using a rope and a bag. Video of each rockfall was captured perpendicular to the rock path and facing the rock path using hand-held cell phone cameras.

Figure 3. The rock cut in Derry, NH, showing Rock Remediation Technicians from Ameritech Slope Contractors pulling the experimental rock up the slope.

The data obtained from experiments at the Derry location include rock stopping location relative to the base of the rock cut, which used to approximate runout distance, as well as acceleration and rotational velocity from the SR for four of the seven tests. Analysis of the video of each rockfall included confirmation of the landing locations of each rock, approximations of bounce heights, and observations of rock motion after impacting the ground.

2.2.2. Results

Runout distances for experimental rockfalls at the Derry rock cut are provided in Table 4. All values are referenced to the base of the rock cut, where the rock talus forming the ditch intersected the slope. The stopping location of each rockfall trial was recorded approximately in the field and checked with analysis of video recordings.

Table 4. Rock runout from Derry, NH from the trials with SR data

Trial	Rock	Approx. Stopping Location (m)	Remark
1	1	4	
2	1	4	
3	1	5.4	
4	2	3.5	No SR data
5	2	3.5	No SR data
6	2	8	No SR data
7	2	4.2	

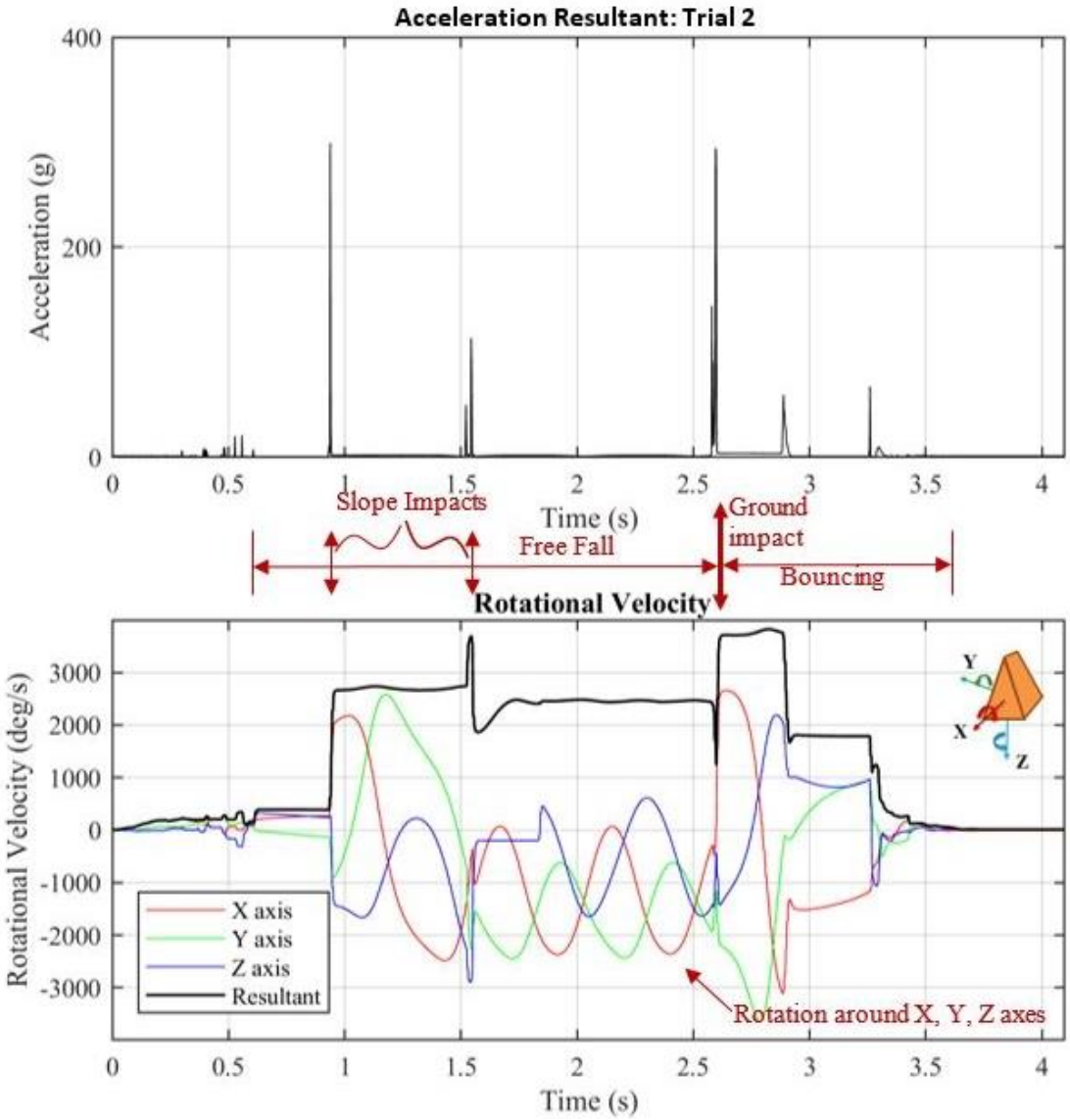

Figure 4. SR results for Derry trial 2, using the approximately 5 kg rock. Top: the resultant acceleration of the rock. Bottom: Rotational velocity as recorded by the SR around individual axes, and the resultant rotational velocity. An approximation of the rock shape is shown to indicate orientation.

Table 5 presents the maximum accelerations and average and maximum rotational velocities for the four SR trials in Derry, NH. The experiment with the approximately 11 kg rock 2 experienced a higher maximum acceleration and slower rotation than the three trials with rock 1. In trials 3 and 7, the maximum capacity of the instruments were exceeded.

Graphical results for trials 2 and 7 are presented in Fig. 4 and Fig. 5, respectively. The motion of the rock can be interpreted from the SR results. During trial 2 with rock 1, shown in Fig. 4, the rock slid at approximately time 0.5 s before falling from the top of the rock cut. It impacted a ledge on the slope at 0.9 s, producing a g-force of 299 g and greatly increasing the rotation of the rock from 388 dps to 2675 dps. The rock then glanced off the slope again just after 1.5 s, which is suggested by a double peak in the acceleration that has a maximum of 113 g, before hitting the ground and experiencing 294 g during deceleration. The rock bounced again several times before stopping at the far edge of the rock-lined ditch at the bottom of the slope.

Table 5. Smart Rock data summary for the experimental trials in Derry, NH.

Trial	Rock	Maximum Resultant Acceleration (g)	Average Resultant Rotational Velocity (dps)	Maximum Resultant Rotational Velocity (dps)
1	1	355	853	2671
2	1	299	1528	3823
3	1	397*	1390	4989*
Average (Trials 1-3)		350	1257	3828
Standard Deviation (Trials 1-3)		49	357	1159
7	2	430*	883	3325

*Approximate number. An individual data axis recorded data at the maximum capacity of the accelerometer or gyroscope.

Trial 2 experienced its maximum acceleration at its first bounce off the slope; corresponding to an approximate impact force of 18 kN. The direction of the force is not known from the SR data, because the SR lacks a stable frame of reference, and therefore, results

cannot currently be corrected for the effect of gravity. However, the data may be used to indicate the approximate magnitude of the forces any barrier on the slope may have to withstand.

During free fall as well as during bouncing after impact, the rock was rotating around all three axes, which can be seen by approximately equal rotational velocities around the X and Y axes between 1.5 s and 2.5 s and slightly lower but still variable rotational velocities around the Z axis.

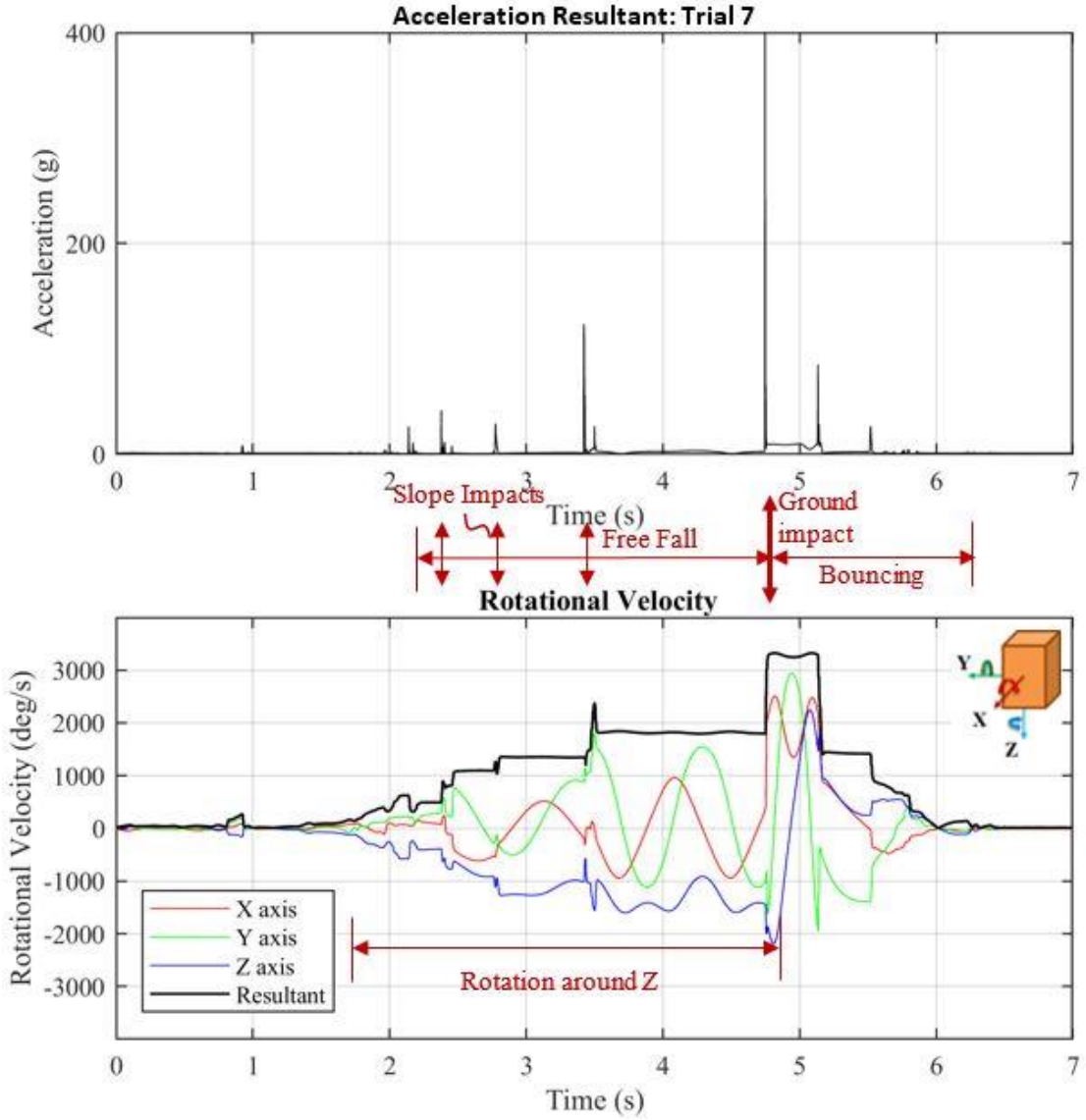

Figure 5. SR results for Derry trial 7 using the approximately 11 kg rock. Top: the resultant acceleration of the rock. Bottom: Rotational velocity as recorded by the SR around individual axes, and the resultant rotational velocity. An approximation of the rock shape is shown to indicate orientation.

Trial 7, using rock 2, was also in free fall for most of the trial. The rock was dropped at approximately 1.2 s and rotated and slid down the rock face until it fell at 2.2 s. It impacted the slope at approximately 2.8 s and 3.4 s, then hit the ground at 4.7 s with a g force that reached or exceeded the 400 g capacity of the instrument. It bounced several times and landed outside of the ditch. As in all of the experiments at this location, the rotational velocity was highest during the bounce after the first impact with the ground. In free fall with rock 2, rotation primarily occurred around the Z axis, which has the smallest moment of inertia, as shown in Fig. 5.

2.3. Hart's Location, NH

2.3.1. Rock cut and experimental procedure

Four experimental rockfalls were conducted at an existing rock cut in Hart's Location, NH. The rock cut is approximately 270 m long at the far northern end of Crawford Notch State Park. The rock face is up to 29 m high and in some places has as little as 1 m between the rock and the edge of pavement. No engineered catchment ditch exists, and the roadway has no shoulder. Two tests were performed at each of the locations shown in Fig. 6.

The test rockfalls were conducted during hand scaling activities in May 2018. SR data were obtained for two of the four experiments, and all tests were

performed with rock 2 due to time limitations. The SR was inserted and started on the ground, and the scalers pulled the test rock up the rock face in a bag for each test. Video footage was taken using hand-held cell phone cameras from behind a concrete barrier facing the fall locations, due to safety restrictions. Traffic was stopped during each rockfall. The stopping location of the SR relative to the rock face was measured for each test.

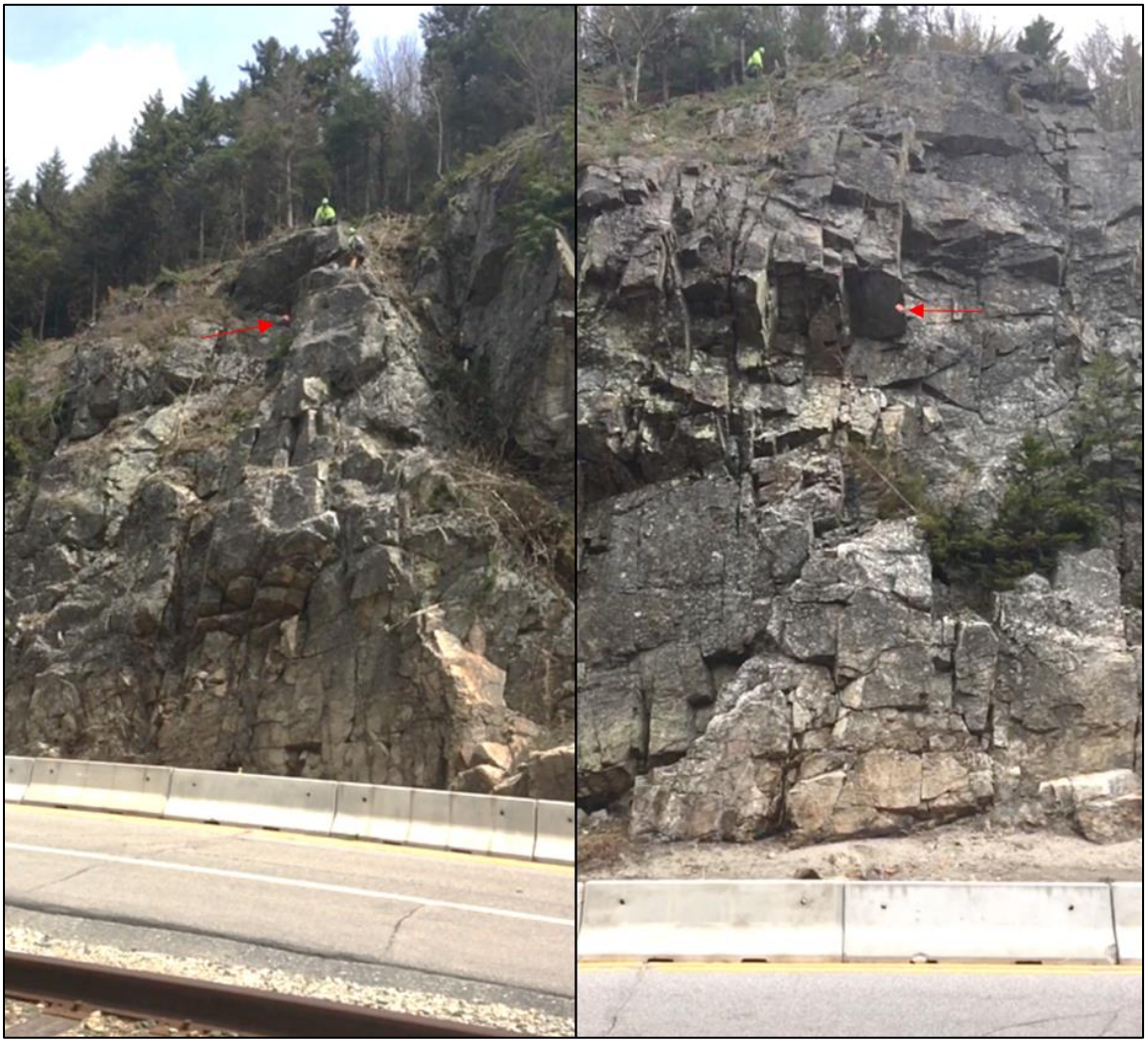

Figure 6. Rockfall tests at Hart's Location, NH. The red arrows indicate the location of the falling rock. Left: Location 1. Right: Location 2.

2.3.2. Results

The rock stopping points, relative to the base of the rock face, for all four trials at Hart's Location are given in Table 6. Because the full trajectory was obscured by barriers for safety, it is not known for all tests if these are true runout values, meaning the farthest points reached by the rock, or if the rocks bounced back towards the slope from their point of impact. Both tests from location 1 are known to have bounced back from their farthest measurement.

Table 6. Runout distances from Hart's Location trials.

Trial	Rock	Drop Location	Stopping Location (m)	Remark
1	2	1	0	Stopped at the base of the rock cut.
2	2	1	5.8	Bounced off centerline barrier. No SR data.
3	2	2	4.7	Impacted and damaged road. No SR data.
4	2	2	4.0	Stopped directly on curb.

Two successful tests of the SR were obtained at Hart's Location, for which the data are summarized in Table 7. The rotational velocities are consistent with values experienced by this rock at the Derry location. The maximum accelerations are estimates only, as the acceleration exceeded the 400 g limit of the high-g accelerometer upon impact with the ground in both trials.

Table 7. Smart Rock data summary for experimental trials at Hart's Location

Trial	Maximum Resultant Acceleration (g)	Average Resultant Rotational Velocity (dps)	Maximum Resultant Rotational Velocity (dps)
1	410*	831	3318
2	621*	951	2049
Average	515*	891	2683

*Approximate number. An individual data axis recorded data at the maximum capacity of the accelerometer or gyroscope.

The data are presented graphically in Fig. 7 and Fig. 8. Unlike previous data shown, all X, Y, Z acceleration data are shown for these tests, because the low-g

accelerometer failed upon impact with the ground at 5.4 s in trial 1. Therefore, the acceleration signal at low g values is incorrect after this point in trial 1, which also affects the resultant acceleration. Recalibration of the instrument for the subsequent trials appears to have fixed the issue, and the data for trial 4 appear normal. The resultant acceleration is shown as a dotted line in the uppermost acceleration plot.

As was seen in Derry with this rock, most of the rotation of the rock appears to be around a single axis in one direction. In trial 1 (Fig. 7), the rock bounced down the slope, moving with less than 1000 dps and changing the rotational velocity with each bounce. Between 1 s and 2.7 s, the rock was rolling and bouncing. The maximum acceleration the rock experienced on the upper slope was 81.4 g, corresponding to an approximate force of 9 kN. At 2.7 s it went into free fall, and at 3.5 s it bounced off a ledge and was launched up and out, which was observed on the video. After approximately one second of free fall, during which it was rotating around the Z axis at approximately 2000 dps, the rock glanced off the slope then fell the remainder of the way, experiencing at least 400 g deceleration and a force of approximately 44 kN upon impact with the ground. The rotational velocity data confirm that the rock moved after impact; the abrupt change in the direction of spin upon impact seen in the individual axis velocities indicate that it likely bounced backwards from its point of impact, towards the slope.

In trial 4, shown in Fig. 8, the rock bounced and rolled down the upper portion of the slope between 0 and 3.8 s. The rotation data confirm that it was primarily rotating around the X axis, which has the highest mass moment of inertia. The highest acceleration it experienced on the upper slope was 91.5 g, corresponding to an approximate force of 10 kN. At 3.8 seconds, it fell from the overhanging rock, again experiencing a resultant rotational velocity of approximately 2000 dps, primarily due to 1500 dps rotation around the Z axis, which has the smallest moment of inertia. It hit the ground at approximately 5.8 s with a resultant acceleration of at least 600 g and a force of approximately 66 kN; again, the accelerometer exceeded its limit. The point of first impact was not observed, but the data confirm that the rock continued moving after impact.

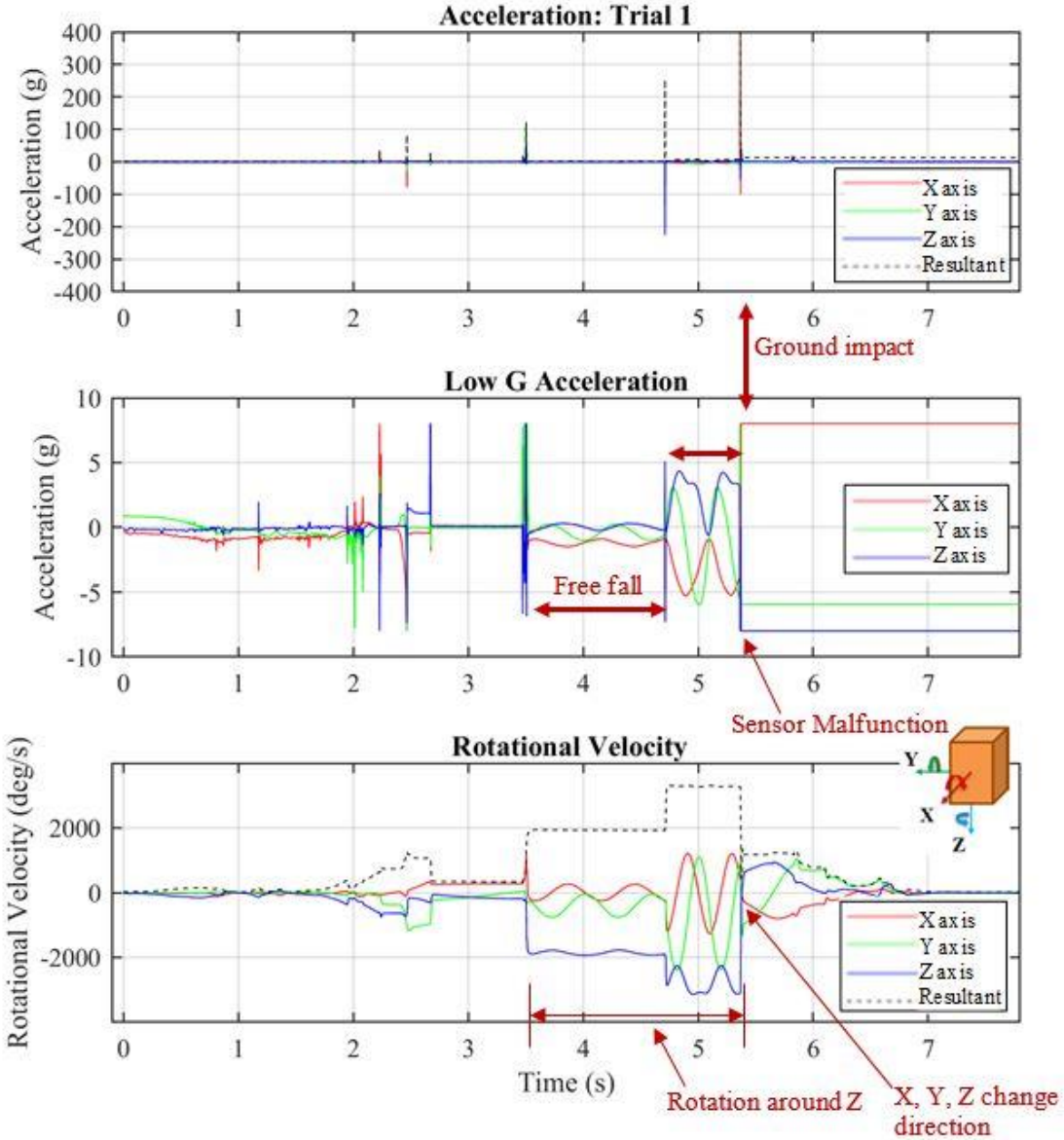

Figure 7. SR data for Hart's Location location 1, trial 1. Top: Data from the ±400 g accelerometer. Center: Data from the ±8 g accelerometer. Bottom: Rotational velocity

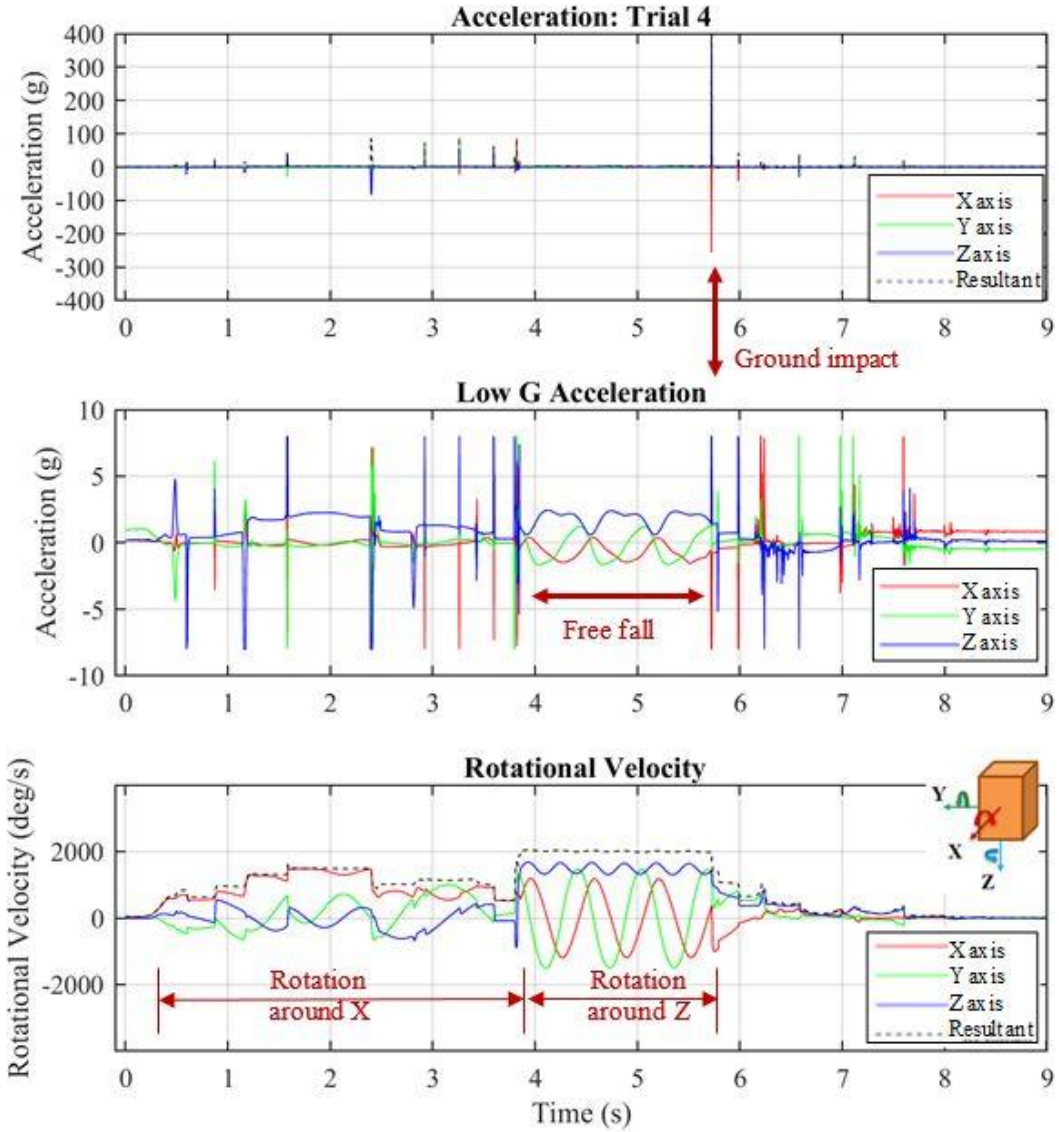

Figure 8. SR data for Hart's Location location 2, trial 4. Top: Data from the ±400 g accelerometer. Center: Data from the ±8 g accelerometer. Bottom: Rotational velocity.

3. Comparison to RocFall Models

3.1. Derry, NH

Rockfall simulations were performed using the software RocFall, using a surface model created from basic photogrammetry as described in section 1.2 [11]. The coefficients of restitution used are presented in Table 1 [18]. Rocks 1 and 2 were simulated by approximating the shape, mass, and density of the rock in the RocFall program (Table 2). 50 trajectories of each of the simulated rocks were dropped from the same location on the simulated slope. The model results, showing simulated trajectories and rock stopping locations, are shown in Fig. 9 and Fig. 10, respectively.

The trajectories modeled generally agree with trajectories observed in the field, which were confirmed with video recordings. Video recordings show that when the test rocks bounced from the rock face, they continued a downward trajectory and first impacted the ground before the lowest point of the ditch. The rocks did not rebound significantly after impact with the ground; most remained close to the surface. The highest bounce after ground impact was less than 1 m in the field experiments; Fig. 9 shows that the simulations often overestimated bounce heights.

Rock stopping locations were recorded in the field with the intention of attempting model calibration using experimental runout data. However, there were too few experimental trials to attempt calibration of the model, and therefore the data were used for direct comparison. Experimental rock stopping locations approximated in red on Fig. 10. Bins for the histograms used here are 0.52 m wide. Simulated rocks were more likely to stop before or run out further than the experimentally measured rock ending locations, which are shown in red on Fig. 10.

Fig. 11 presents the rotational velocity data output from the experimental trials with the SR compared to average values from the computational model. Results from a second model set are also shown, which used higher coefficients of restitution chosen from the literature for a comparison discussed further in [11]. This graph shows all four trials using the SR, with time

from the SR used as a proxy for the position of the test rock on the slope, because no location data are available for the experimental trials. The predicted average rotational velocities during free fall are close to what is observed using the SR.

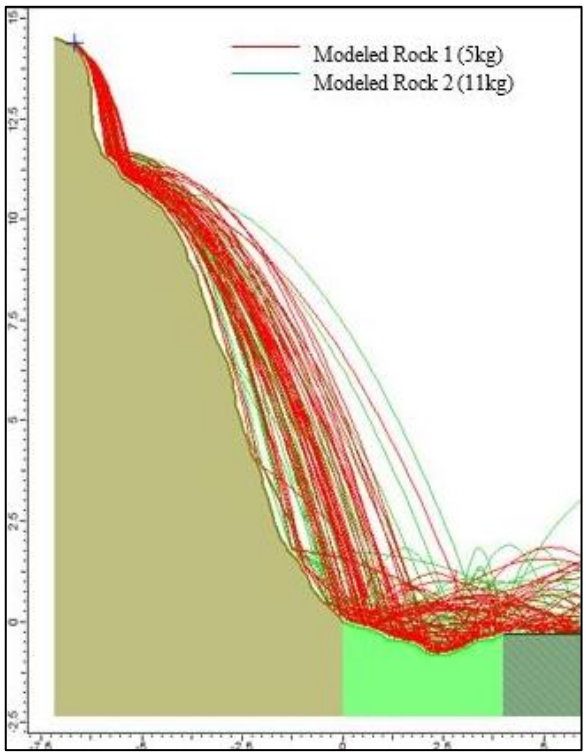

Figure 9. Trajectory simulations for the Derry rock cut. Colors represent surface materials described by the coefficients of restitution in Table 1.

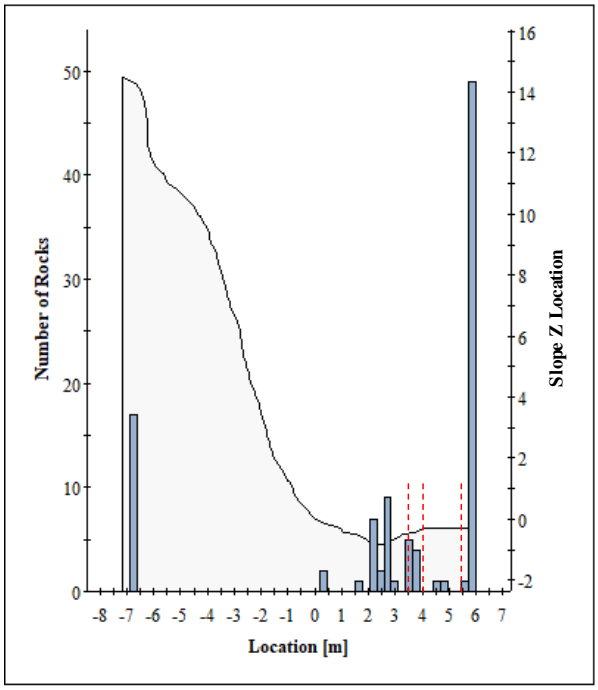

Figure 10. Output from RocFall showing rock ending locations for Derry simulations.

Free fall can be identified in all of the data sets in Fig. 11 where the rotational velocity is constant. The modeled data, because it is averaged from 100 simulations (50 for each rock type), does not show peaks in rotational velocity representing impacts with the slope. These are visible in the SR data accompanied by a shift in the rotational velocity. The average rotational velocities predicted by both models in free fall, from approximately -5 m to -1 m, are between 1750 dps and 2000 dps. The SR trial with the rock 2 is very similar at approximately 1750 dps during free fall between 1 s and 3 s. Other measured velocities in free fall range from 1000 dps to nearly 3000 dps, indicating that the predicted 2000 dps average is very reasonable.

After impact with the ground, the SR measured increased rotation in all trials as the rock bounced, up to or exceeding 4000 dps. The averaging applied to the modeled data mutes any extremes that might have occurred in individual simulated trials, but there is an increase visible in Fig. 11 once the rock impacts the ground, and the rotation gradually climbs to 3000 dps. However, though 3000 dps is comparable to measured rotations immediately after ground impact, after the first bounce off the ground the SR recorded a decreasing trend in rotational velocity in all four trials. The increasing rotational velocity suggested by the models is a result of the large number of simulations in which the rock ran out past the edge of the model; rocks that were rotating more slowly appear to have stopped closer to the rock cut, so the average rotational velocity increased as the number of simulated trajectories being averaged decreased. While it is possible that between 2 m and 6 m a few rocks might reach the rotational velocities predicted by the model, based on the experimental data from the SR, it is unlikely that many would do so. The sharp drop in modeled average rotational velocity at approximately 6 m indicates the edge of the modeled data and corresponds with the large number of rocks "ending" at this location in Fig. 10.

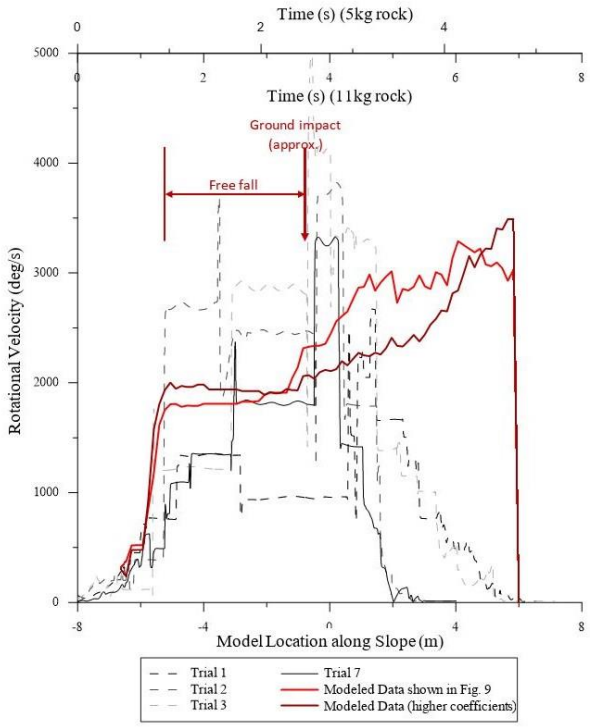

Figure 11. Comparison of average modeled values to measured rotational velocities, Derry

3.2. Hart's Location, NH

A photogrammetry model of the rock cut a Hart's Location was provided by the NHDOT. Slope profiles were extracted from this surface to simulate the slope for rockfall models. The locations of these profiles, corresponding to the experimental drop locations, are shown in Fig. 12.

For comparison to the experimental results obtained using rock 2, 50 trajectories were calculated for each experimental location using the simulation of rock 2 in RocFall. Due to tree cover in the photogrammetry model that no longer existed when the SR rocks were dropped, the cross-section used for location 2 is shorter than the actual slope and does not depict the drop point used for field experiments. Due to this, the rock starting location in the location 2 model was placed 0.75 m above the surface, and the simulated rock was given an initial velocity of 1 m/s in the horizontal direction and -1 m/s in the vertical direction.

The coefficients of restitution used to model the Hart's Location rockfalls are presented in Table 1. Fig. 13 and Fig. 14 show the modeled trajectories for each of the two experimental locations, with the measured rock ending points shown in red on each figure. With only two experimental rockfalls per location, it is not possible to draw definite conclusions from these figures, but in both cases, modeled results do predict that some simulations will land in the same approximate locations as the experimental trials. At location 1, one of the experimental rockfalls was observed to bounce off the barrier placed on the center line of the road, at approximately 7 m from the base of the slope. This suggests that without the barrier, it would have traveled farther. Therefore, the modeled prediction from both locations that many rocks will travel across the roadway cannot be discounted.

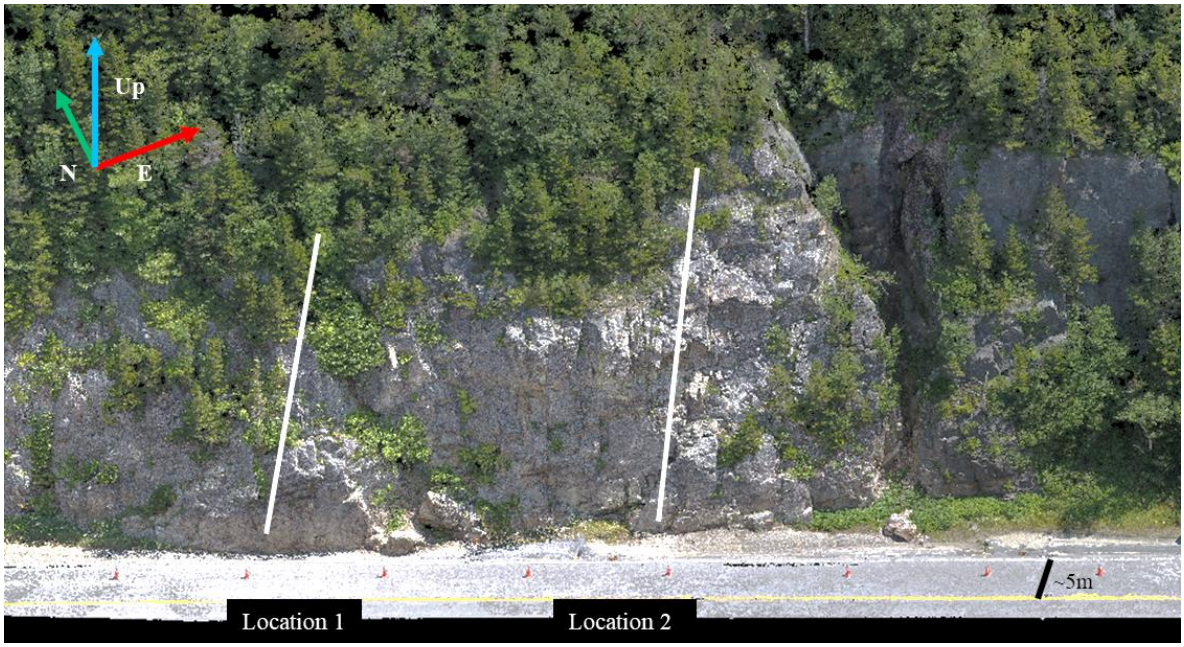

Figure 12. Model of the Hart's Location rock cut and cross-section locations.

Based on video from the Hart's Location trials, some of the bounce heights predicted by both models are probably high. The bounce after the rock hit the roadway was visible over the approximately 1 m tall concrete barrier on the road in only one trial. It is therefore unlikely that many rocks would reach heights of 2.5 m after impact, as predicted by the computational models. This suggests that the coefficient of restitution in use for asphalt in the simulation may be too high. Some modeled trajectories predicted that the rocks would remain closer to the ground surface, which is more reasonable based on the field experiments. In one field test, the test rock penetrated the asphalt, which is not accounted for in the computational model.

Fig. 15 and Fig. 16 present average rotational velocity data for each simulated location from Hart's Location compared to the measured rotations for the one successful SR test at each location. Time is used as a proxy for horizontal location on the slope for the SR data. Though the time and location data cannot be inferred to overlap exactly as depicted, in Fig. 15 the average rotational velocities correlate well with the measured SR data. In free fall at location 1, the SR experienced rotational velocities of approximately 400 dps, 2000 dps, and 3400 dps. Based on these numbers, the average modeled values between 1000 dps and 2000 dps during the time the simulated rocks are in free fall, between approximately -4 m and 4 m, appear reasonable.

In Fig. 16, showing the measured and modeled rotational velocity results from location 2, the data again correlate well while the rock is on, or falling from, the slope. On this plot, the average result from the computational model is shown as a solid red line. The impact of the rock with the ground is labeled for both the SR data and the simulated results. Here, the averaged model data show the impact more clearly than at location 1, because the rock trajectories are less variable, as seen in Fig. 14. Both the measured and modeled data show rotational velocities increasing from 0 to 1500 dps when the rock is rolling down the slope, then reaching 2000 dps in free fall.

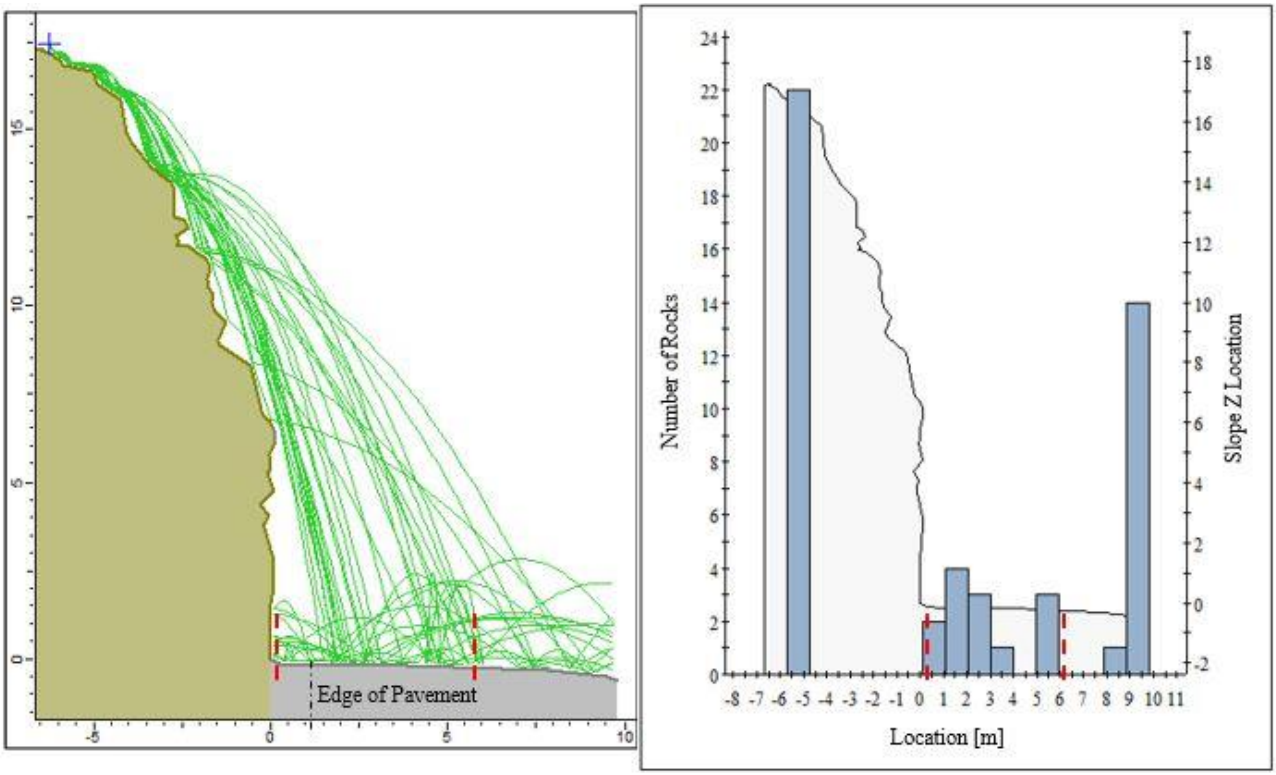

Figure 13. Trajectory model (left) and modeled rock path end points (right) for the Hart's Location experimental rockfall at location 1. Experimental ending locations of the SR trials are shown in red.

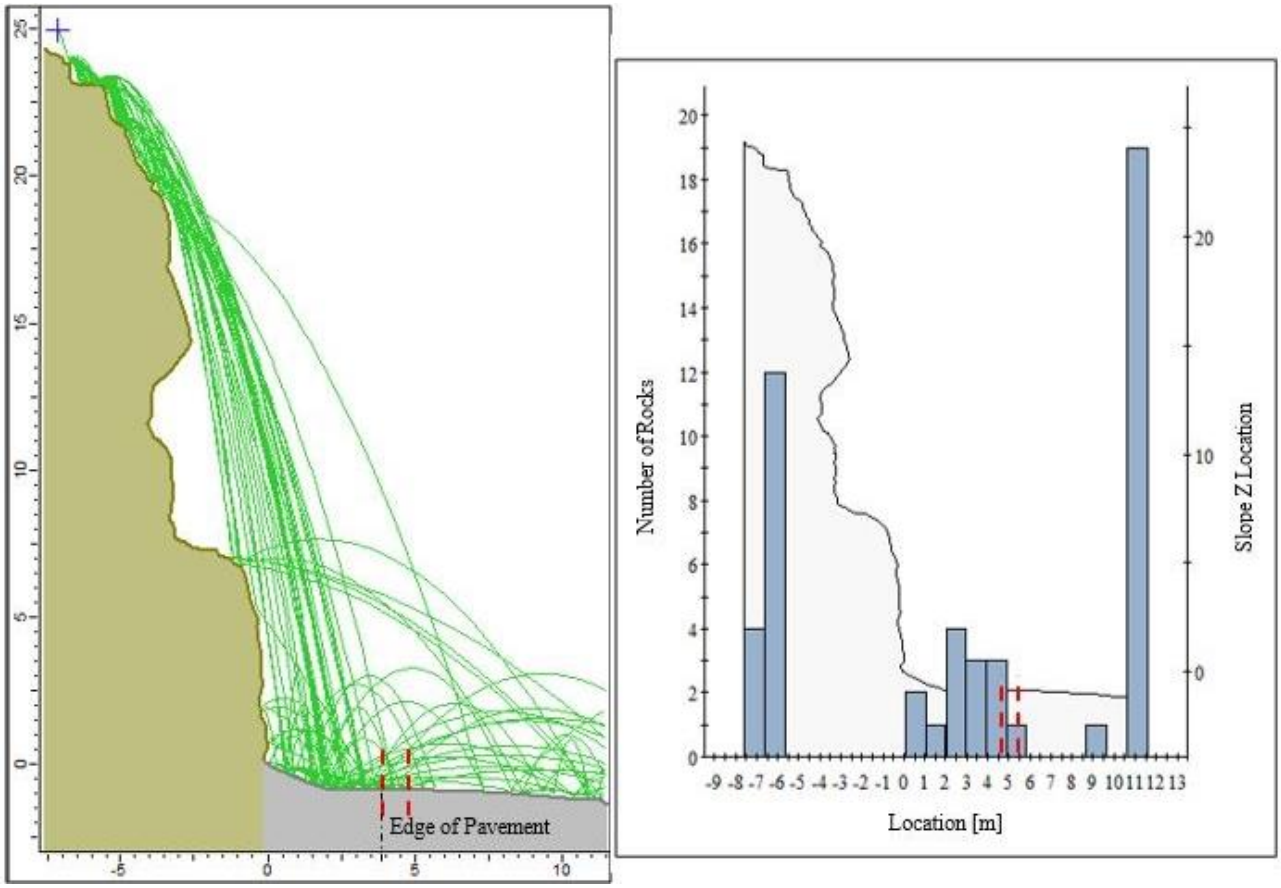

Figure 14. Trajectory model (left) and modeled rock path end points (right) for the Hart's Location experimental rockfall at location 2. Experimental SR rock end points are shown in red.

The experimental and modeled data shown in Fig. 15 and Fig. 16 sharply diverge upon impact of the rocks with the ground; the SR shows that the rock experienced a large decrease in rotational velocity after impact, which continued in a decreasing trend until the rock stopped moving. The modeled data predict a large increase in rotational velocity after impact with the ground, until the average exceeds 4000 dps. Like the Derry models, this is due to the decreasing number of trajectories accounted for in the average allowing a few

quickly-rotating rocks that travel this distance to increase the average rotational velocity. To attempt to correct for this, the dashed red line shows the average if all rock trajectories are included in the calculation, including those that do not reach the location and therefore have a velocity of zero.

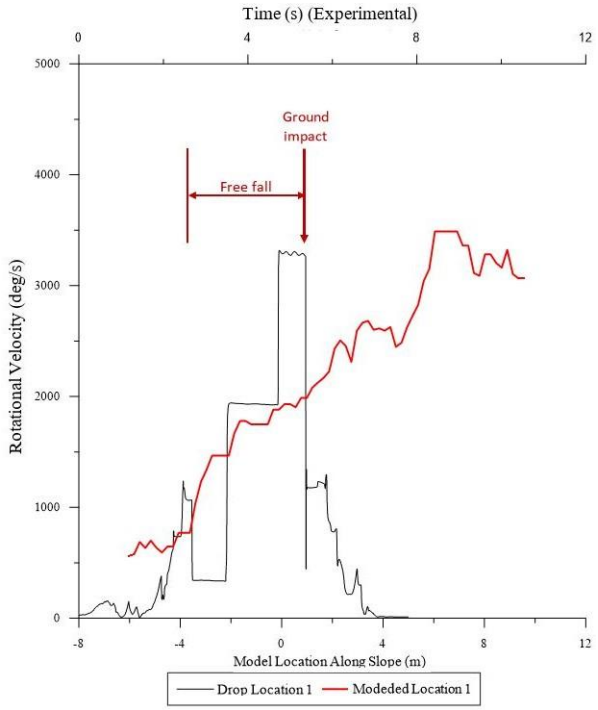

Figure 15. Comparison of averaged modeled versus measured rotational velocity, location 1, Hart's Location.

The standard model output, as was shown in the Derry models, averages only those rocks that pass the location of interest. At 2 m, 43 out of the 50 simulated rocks are included in the average; some having stopped on the upper portion of the slope. At approximately 10 m, only 20 rocks are included in the average by the RocFall software. By including the results of all 50 simulations, the dashed line on Fig. 16 may provide a more realistic view of the rotational velocity of a rock at any one location, though it is a less conservative approach. The rotational velocities in this plot are lower than the standard model output because of the inclusion of the trajectories that represent a velocity of zero, i.e.: the rock had stopped prior to the measured point. The calculated average rotational velocities remain in general agreement with the measured SR data from the single experimental trajectory. Because it is expected that some rocks would continue to run out farther than was observed in the experiment, the rotational velocities after the impact with the ground remain high, but the decreasing trend observed in the corrected data is more realistic, compared against experimental observations, than the increase seen in the standard model output.

The accuracy of the predicted rock stopping locations in these models cannot be determined from the available data, except to say that they do not disagree with the few available experimental tests. Though basic models were run using program default coefficients of restitution (Table 1), the rotational velocities predicted in general agree with measured SR data. As in Derry, the accuracy of the modeled rotational velocities from the model output after the simulated rock reaches the bottom of the slope are in doubt. The model predicts much faster velocities than were observed. A manual correction of the data to include rotational velocities from all simulated rock trajectories, including those no longer moving at a given horizontal location, shows somewhat better agreement with the experimental data and provides a more realistic view of potential rock motion.

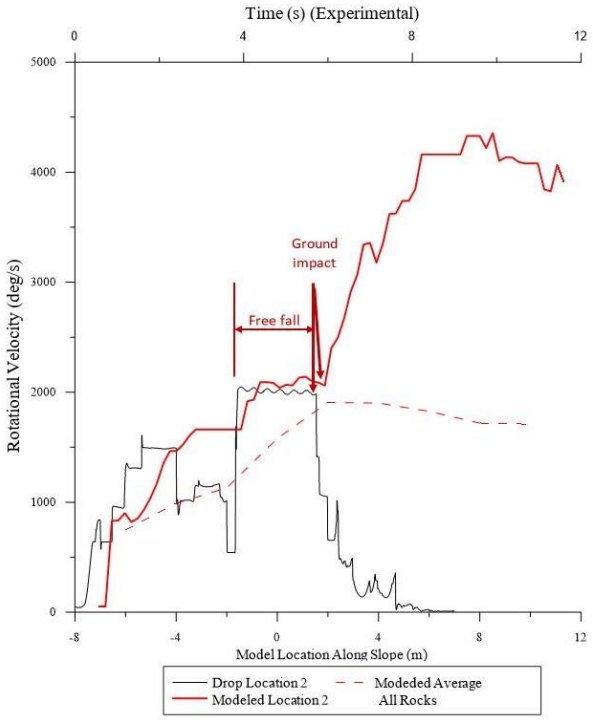

Figure 16. Comparison of average modeled versus measured rotational velocity, location 2, Hart's Location.

4. Discussion

4.1. Smart Rock

Translational and rotational velocities are very important for energy and impact analyses, as they are major influences on kinetic energy [7, 13, 14]. Acceleration can be used to calculate the force at which a rock impacts a surface or a barrier [20]. Being able to take direct measurements of rock motion can be very useful for estimating the effect a falling rock will have and for properly designing protection measures. Though the forces estimated from the current SR are not corrected for the influence of gravity due to the lack of a known spatial reference system, the calculations can be used to inform models or to design a barrier for the worst-case scenario. Also, the large difference in accelerations and forces at the top of the Derry and Hart's Location slopes compared to the forces with which the rock hit the ground could provide information on where it might be best to place a barrier, or the type of barrier that should be used.

Rockfall runout and rotational velocity were the data of interest for this study, to use for comparison to modeled rockfall simulations. The rotational velocity results from this study align with measured rotational velocities published by [8 and 9], which included

maximum rotations between 2500 and 4500 dps, despite significant differences in the experimental slopes and procedures.

The SR data can also be used to infer the motion of the rock. The differences in the SR output for the two different rock shapes generally agrees with results of rock shape on rotation reported by [9]. Caviezel et al. [9] found that their rocks stabilized into rotation around the "largest axis of inertia" in all of the rock shapes they tested, unless the rocks were "heavily elongated." In this experiment, rock 1, with an elongated shape, tended to rotate around multiple axes during falling and rolling, as seen demonstrated by the SR data in Fig. 4. The one example reported for a similar rock shape by [9] similarly experienced significant rotation around the X and Z axes.

Rock 2 stabilized to rotate primarily around a single axis in every trial regardless of experimental location. In both Derry and Hart's Location, it stabilized around the Z axis during free fall, which has the lowest moment of inertia (Table 3), which can be seen in Figs. 5, 7, and 8. This appears to be a function of the type of motion the rock experienced moving down the slope. Rotation around the Z axis, with the smallest moment of inertia, occurred while the rock was in free fall, as compared to results from [9], which were produced on a shallower slope on which the rock rolled. This is most easily seen in Fig. 8; the rotation axis changed from X to Z at 3.8 s, when the rock motion changed from rolling and bouncing to free fall.

Though the magnitudes are comparable to published values, the raw SR measurements from the 11 kg rock may not be fully accurate in describing rock motion. The SR was offset from the center of mass inside the natural rock, and this eccentricity will have affected the acceleration and rotational data. This is not explored here.

4.2. Model Comparisons

2D rockfall models were created for the rock slopes in Derry and Hart's Location, NH that were used for Smart Rock experiments. The results of the computational models were compared to experimental data in order to determine if readily-available digital data, such as the photogrammetry models used here, could be used to accurately simulate rockfalls. Experimental data used for comparison included measured rock runout, approximate observed trajectory bounce heights, and the measured rotational velocity of the test rocks. From these models and comparisons, it is shown that photogrammetry models created with readily-available resources, which represent the shape and roughness of the slope of interest, simulate rockfalls with realistic motion of the rock. It is also shown that models created using the default coefficients of restitution in the RocFall program can predict realistic rock motion and rotation, as seen in the presented models when compared to field observations and Smart Rock data.

5. Conclusions

This research shows that the University of New Hampshire's rockfall Smart Rock, placed inside a real rock, accurately records the acceleration and rotational velocity of the falling rock. These measurements from a Smart Rock can be used to describe the motion of a rock throughout its fall down a slope, and can also be used to verify modeled rock motion and rotational velocity.

Acknowledgements

Acknowledgements to the New Hampshire Department of Transportation Bureau of Materials and Research for facilitating and conducting the field experiments, and to Ameritech Slope Contractors for their assistance with the experiments. Also acknowledgements to the NHDOT and University of Vermont for photogrammetry data, and to the University of New Hampshire for support of this work, including to John Ahern for rock preparation.

References

[1] Pierson, L.A., Gullixson, C.F., and Chassie, R.G. "Rockfall Catchment Area Design Guide", Oregon Department of Transportation, Salem, Oregon, USA, Rep. FHWA-OR-RD-02-04m, 2001.

[2] Duffy, J.D. and Turner, A.K. "Conducting Field-Test Experiments." In: Turner, A.K. and Schuster, R.L. (eds) Rockfall Characterization and Control, Transportation Research Board, Washington, D.C., USA, 2012, pp. 407-441.

[3] Apostolov, A. "Development and testing of motion tracking "Smart Rock" devices for geotechnical applications", Master's thesis, University of New Hampshire, 2016.

[4] Gullison, M. "Analysis of Smart Rock data from debris flow experimentation", Master's thesis, University of New Hampshire, 2013.

[5] Harding M., Fussell B., Gullison M., Benoit J., and de Alba P. "Design and testing of a debris flow 'Smart Rock'", Geotechnical Testing Journal, 37(5), pp. 769-785, 2014. https://doi.org/10.1520/GTJ20130172

[6] Apostolov, A. and Benoît, J. "Motion Tracking 'Smart Rock' Device for the Study of Landslide and Debris Flow Mechanisms", In: North American Symposium on Landslides, Roanoke, VA, USA, 2017, pp. 889-900.

[7] Wyllie, D.C. "Rock Fall Engineering", 1st ed., CRC Press, Taylor & Francis Group, New York, NY, USA, 2015.

[8] Caviezel, A., and Gerber, W. "Brief communication: measuring rock decelerations and rotation changes during short duration ground impacts", Natural Hazards and Earth System Sciences Discussion, *in review* 2018. https://doi.org/10.5194/nhess-2018-89

[9] Caviezel, A., Schaffner, M., Cavigelli, L., Niklaus, P., Bühler, Y., Bartelt, P., and Magno, M. "Design and evaluation of a low-power sensor device for induced rockfall experiments", ISEE Transactions on Instrumentation and Measurement, 67(4), 2018. https://doi.org/10.1109/TIM.2017.2770799

[10] Harding, M. (2011). Design and development of a debris flow tracking "Smart Rock". (Master's thesis). University of New Hampshire, Durham, NH.

[11] Disenhof, C. "Investigation of Surface Models and the Use of a Smart Rock for Rockfall Modeling", Master's thesis, University of New Hampshire, 2018.

[12] Rocscience, "RocFall" (6.0) [computer program]. Available at: rocscience.com [Accessed: 2017].

[13] Ashayer, P. "Application of rigid body impact mechanics and discrete element modeling to rockfall simulation", Doctoral thesis," University of Toronto, 2007.

[14] Turner, A.K., and Duffy, J.D. "Evaluation of Rockfall Mechanics", In: Turner, A.K. and Schuster, R.L. (eds). Rockfall

Characterization and Control, Transportation Research Board, Washington, D.C., USA, 2012, pp. 285-333.

[15] Chai S., Yacoub, T., Charbonneau, K., and Curran, J.H. "The effect of rigid body impact mechanics on tangential coefficient of restitution," In: GeoMontréal 2013, Montreal, Canada, 2013.

[16] Dadashzadeh, N., Duzgun, H.S.B., Yesiloglu-Gultekin, N., and Bilgin, A. "Comparison of lumped mass and rigid body rockfall simulation models for the Mardin Castle, Turkey", In: 48th US Rock Mechanics & Geomechanics Symposium, American Rock Mechanics Association, 14(7177), Minneapolis, MN, USA, 2014.

[17] Rocscience, RocFall Help. "Coefficient of Restitution", [online] Available at: https://www.rocscience.com/help/rocfall [Accessed: July 2017].

[18] Rocscience, RocFall Help. "Coefficient of Restitution Table", [online] Available at: https://www.rocscience.com/help/rocfall [Accessed: July 2017].

[19] New Hampshire Department of Transportation. "New Hampshire Rock Cut Database", Unpublished. [Accessed 18 January 2018].

[20] Nelson, G.S. and Snowden, T.D. "Physics Calculations Related to Falling Objects", Nelson & Associates, Bryan, TX, USA, 2010. https://doi.org/10.13140/RG.2.1.3596.5522